Psychological stress activates a dorsomedial hypothalamus-medullary raphe circuit driving brown adipose tissue thermogenesis and hyperthermia.

AUTHOR(S):

Kataoka, Naoya; Hioki, Hiroyuki; Kaneko, Takeshi; Nakamura, Kazuhiro

CITATION:

Kataoka, Naoya ...[et al]. Psychological stress activates a dorsomedial hypothalamus-medullary raphe circuit driving brown adipose tissue thermogenesis and hyperthermia.. Cell metabolism 2014, 20(2): 346-358

ISSUE DATE:

2014-08-05

URL:

http://hdl.handle.net/2433/194291

Psychological Stress Activates a Dorsomedial Hypothalamus–Medullary Raphe Circuit Driving Brown Adipose Tissue Thermogenesis and Hyperthermia

Naoya Kataoka,[1] Hiroyuki Hioki,[2] Takeshi Kaneko,[2] and Kazuhiro Nakamura[1,3,*]

[1]Career-Path Promotion Unit for Young Life Scientists

[2]Department of Morphological Brain Science, Graduate School of Medicine

Kyoto University, Sakyo-ku, Kyoto 606-8501, Japan

[3]PRESTO, Japan Science and Technology Agency, Kawaguchi, Saitama 332-0012, Japan

*Correspondence: kazu@cp.kyoto-u.ac.jp or nkazuhir@gmail.com

Running Title: Neural Circuit for Stress-Induced Hyperthermia

SUMMARY

Psychological stress-induced hyperthermia (PSH) is a fundamental autonomic stress response observed in many mammalian species. Here we show a hypothalamomedullary, glutamatergic neural pathway for psychological stress signaling that drives the sympathetic thermogenesis in brown adipose tissue (BAT) that contributes to PSH. Using *in vivo* drug nanoinjections into rat brain and thermotelemetry, we demonstrate that the rostral medullary raphe region (rMR) and dorsomedial hypothalamus (DMH) mediate a psychosocial stress-induced thermogenesis in BAT and PSH. Functional neuroanatomy indicates that the DMH functions as a hub for stress signaling, with monosynaptic projections to the rMR for sympathetic outputs and to the paraventricular hypothalamic nucleus for neuroendocrine outputs. Optogenetic experiments showed that the DMH–rMR monosynaptic pathway drives BAT thermogenesis and cardiovascular responses. These findings make an important contribution to our understanding of the central autonomic circuitries linking stress coping with energy homeostasis—potentially underlying the etiology of psychogenic fever, a major psychosomatic symptom.

HIGHLIGHTS

• DMH and rMR neurons mediate stress-induced BAT thermogenesis and hyperthermia

• DMH functions as a hub for stress signals to sympathetic and neuroendocrine outputs

• Photostimulated DMH–rMR neurotransmission drives autonomic responses mimicking stress

• LH–rMR projection neurons including orexin neurons elicit only weak BAT thermogenesis

INTRODUCTION

Psychological stress is mental strain or pressure under the perception of impending endangerment, pain or discomfort and triggers various physiological responses. Many psychological stressors induce an acute elevation of body temperature, which is called psychological stress-induced hyperthermia (PSH). Although PSH is a fundamental autonomic stress response observed in many mammalian species, its central circuitry mechanism has yet to be determined. The development of PSH presumably increases physical and neural performances through warming up muscles and the central nervous system by a few degrees Celcius (Bishop, 2003)—beneficial in surviving the "fight or flight" situations when animals confront enemies. In humans, however, intense, long-lasting psychological stress often causes chronic hyperthermia, which is recognized as a major psychosomatic symptom called "psychogenic fever" (Timmerman et al., 1992; Oka and Oka, 2012). Many clinical cases of "fever of unknown origin" (exhibiting no abnormality in diagnostic tests nor physical examination except high body temperature) are found psychogenic (Nozu and Uehara, 2005). Distinct from inflammation-induced fever, PSH and many cases of psychogenic fever are resistant to cyclooxygenase inhibitors (Vinkers et al., 2009; Lkhagvasuren et al., 2011; Oka and Oka, 2012), indicating that PSH does not involve central pyrogenic triggering by prostaglandin E_2 (PGE_2) (Nakamura 2011; Saper et al., 2012). For understanding the mechanism of PSH, it is important to determine the central efferent pathways for the stress-driven autonomic signaling that leads to the development of the thermal responses. Elucidating the central neural substrate for PSH would also contribute to understanding the etiology of psychogenic fever.

We have reported that blockade of β_3-adrenoceptors diminishes PSH (Lkhagvasuren et al., 2011). Since the β_3-adrenoceptor is the primary subtype mediating sympathetic thermogenesis in brown adipose tissue (BAT) (Cannon and Nedergaard, 2004), our finding indicates that heat production in BAT makes a major contribution to the stress-induced elevation of body temperature. Psychological stress induces activation of sympathetic premotor neurons in the rostral medullary raphe region (rMR), including the rostral raphe pallidus and raphe magnus nuclei (Lkhagvasuren et al., 2011). Although these sympathetic premotor neurons express vesicular glutamate transporter (VGLUT) 3 and control BAT thermogenesis for fever and cold defense (Nakamura et al., 2004), there is no direct functional evidence that neurons in the rMR mediate stress-induced BAT thermogenesis.

The dorsomedial hypothalamus (DMH) plays a pivotal role in stress-induced cardiovascular and neuroendocrine responses (Stotz-Potter et al., 1996a,b), as well as in febrile and cold-induced BAT thermogenesis (Madden and Morrison, 2004; Nakamura et al., 2005; Nakamura and Morrison, 2007). However, whether neurons in the DMH are involved in the development of PSH is unknown. The DMH provides a direct axonal projection to the rMR (Hosoya et al., 1987). In light of the critical roles of the DMH and rMR in febrile and cold-induced BAT thermogenesis (reviewed in Nakamura 2011), the DMH–rMR monosynaptic pathway might mediate the sympathetic outflow to drive BAT thermogenesis for fever and cold defense. Furthermore, if the DMH and rMR are both involved in stress-induced BAT thermogenesis, this pathway might also contribute to the stress-driven sympathetic outflow to BAT. However, there is a controversial view that a multisynaptic pathway through the ventrolateral part of the caudal periaqueductal gray (vlcPAG) could transmit a BAT thermogenic signal

from the DMH to the rMR (Chen et al., 2002; Yoshida et al., 2005). Furthermore, in addition to DMH neurons, orexin neurons in the lateral hypothalamic area (LH) have also been proposed to contribute to stress-induced BAT thermogenesis (Zhang et al., 2010). A detailed mapping of rMR-projecting, stress-activated neurons in the caudal hypothalamus would allow delineation of the candidate sites that should be targeted in functional studies to identify PSH-mediating neurons.

Here we explicate the roles of the DMH and the rMR in psychological stress-induced BAT thermogenesis and hyperthermia by examining the effects of drug nanoinjections into these brain regions on the thermal responses in rats exposed to social defeat stress, a psychological stress model that is close to human social stress and induces PSH (Björkqvist, 2001; Lkhagvasuren et al., 2011). We also mapped the distribution of rMR-projecting, stress-activated neurons in the caudal hypothalamus and compared with that of stress-activated neurons that project to the paraventricular hypothalamic nucleus (PVH), a neuroendocrine output center. Finally, *in vivo* optogenetic experiments were performed to identify a hypothalamomedullary pathway that drives BAT thermogenic and cardiovascular responses mimicking those induced by stress.

RESULTS

Social Defeat Stress Induces BAT Thermogenesis and Hyperthermia

Temperatures of the interscapular BAT (T_{BAT}) and abdominal cavity (body core temperature; T_{core}) of free-moving rats were simultaneously monitored using telemetric temperature probes. To confirm that this dual temperature recording can detect BAT thermogenesis and hyperthermia, we injected the lateral ventricle with PGE_2, a pyrogenic mediator inducing BAT thermogenesis (Nakamura 2011). T_{BAT} started

to rise immediately after the injection of PGE_2 and increased by 1.7 ± 0.4°C to a peak (peak ΔT_{BAT}, n = 5) within 30 min (Figure S1). T_{core} always started to rise 1–2 min later than the initiation of the T_{BAT} rise and followed the increase in T_{BAT} (peak ΔT_{core}: 1.5 ± 0.4°C; Figure S1). These properties of the changes in T_{BAT} and T_{core} are consistent with BAT heat production during fever being transferred to the rest of the body to elevate T_{core}, and indicate that the observed rise in T_{BAT} preceding the increase in T_{core} reflects BAT thermogenesis.

We then examined the effect of social defeat stress on T_{BAT} and T_{core}. Soon after intruder Wistar rats were placed into the cages of dominant resident Long-Evans rats, the intruders were defeated by the residents and exhibited an increase in T_{BAT} of 2.6 ± 0.2°C (peak ΔT_{BAT} within 60 min of stress period, n = 6; Figure 1A and B). Similar to the PGE_2-evoked responses, T_{BAT} started to rise immediately after the initiation of the stress exposure, and this was followed after 1–2 min by an increase in T_{core} (Figure 1A and B; peak ΔT_{core}: 2.3 ± 0.3°C). To test whether the social defeat stress-induced increases in T_{BAT} and T_{core} are dependent on β-adrenoceptors, we injected the β-adrenoblocker propranolol intravenously prior to the stress exposure. Propranolol significantly reduced the stress-induced increases in both T_{BAT} and T_{core}, compared with saline injection (Figure 1C–F). These results support our view (Lkhagvasuren et al., 2011) that social defeat stress induces sympathetic BAT thermogenesis, which, in turn, supports a major part of the elevation of T_{core} during the development of PSH.

Thermal Responses to Social Defeat Stress Require Glutamatergic Activation of Neurons in the rMR

To investigate the functional contribution of neurons in the rMR to the stress-induced BAT thermogenesis and hyperthermia, we inactivated

neurons in the rMR by nanoinjecting muscimol, a $GABA_A$ receptor agonist that inhibits neurons locally. Injection of muscimol into the rMR (Figure 2A and C) eliminated the increases in T_{BAT} and T_{core} induced by social defeat stress (Figure 2D–G), but did not significantly affect basal T_{BAT} or T_{core} (Table S1). In contrast, stress exposure following saline injection into the rMR induced large increases in T_{BAT} and T_{core}, which were comparable to the stress responses in non-injected rats (Figures 1A and 2D–G).

To determine whether excitatory neurotransmitter inputs to the rMR are involved in stress-induced physiological responses, we blocked glutamate receptors in the rMR prior to the stress exposure by nanoinjecting a mixture of AP5 and CNQX (AP5/CNQX), antagonists for NMDA and AMPA glutamate receptors, respectively (Figure 2B). This injection eliminated most of the increases in T_{BAT} and T_{core} induced by social defeat stress (Figure 2H–K), and also inhibited the tachycardic, but not pressor, response to the stress (Figure S2). These results indicate that glutamatergic activation of neurons in the rMR is an important process in the stress-driven sympathetic signaling to BAT and to the heart during the development of PSH.

Thermal Responses to Social Defeat Stress Are Modulated by Activation of 5-HT_{1A} Receptors in the rMR

Activation of 5-HT_{1A} receptors inhibits BAT thermogenesis evoked by skin cooling or leptin injection and a part of this effect is mediated through their effect(s) in the brain (Morrison, 2004; Nakamura and Morrison, 2007). We examined whether the stress-induced BAT thermogenesis and hyperthermia are affected by activation of 5-HT_{1A} receptors. Subcutaneous injection of 8-OH-DPAT, a 5-HT_{1A} receptor agonist, eliminated the increase in T_{BAT} evoked by social defeat stress

(Figure S3A and B). This systemic injection also caused hypothermia (Figure S3C and D) as reported (Hjorth, 1985).

Since spinally projecting neurons in the rMR express 5-HT_{1A} receptors (Helke et al., 1997), we examined whether activation of rMR 5-HT_{1A} receptors is sufficient to inhibit stress-induced thermal responses. Nanoinjection of 8-OH-DPAT into the rMR (Figure S3G, inset) strongly reduced the increases in T_{BAT} and T_{core} induced by social defeat stress, but did not lower T_{core} below the baseline (Figure S3E–H), in contrast to the hypothermic effect of the systemic injection of 8-OH-DPAT. These results raise the possibility that serotonergic inputs to the rMR or locally released serotonin can inhibit stress-induced BAT thermogenesis and hyperthermia through local 5-HT_{1A} receptors.

Social Defeat Stress-Induced Activation of DMH Neurons Projecting to the rMR and PVH

The critical role of glutamatergic neurotransmission to the rMR in stress-induced BAT thermogenesis prompted us to examine the caudal hypothalamus as a source(s) of the stress-driven thermogenic inputs to the rMR. We also sought to identify caudal hypothalamic neurons providing a stress signal to the PVH, which potentially drives neuroendocrine stress responses. To separately visualize rMR- and PVH-projecting neurons, two types of cholera toxin b-subunit (CTb), a retrograde tracer, conjugated with different fluorophores, Alexa594 and Alexa488, were injected into the rMR and PVH, respectively (Figure 3A and B and Figure S4A and B). The rats were subsequently subjected to social defeat stress and expression of Fos, a marker of neuronal activation (Sagar et al., 1988), was examined in CTb-labeled caudal hypothalamic neurons.

The injection of Alexa594-conjugated CTb into the rMR (rMR-CTb) resulted in retrograde labeling of many neuronal cell bodies in a dorsal part of the caudal hypothalamus (Figure 3E and F) (Hermann et al., 1997). In contrast, neurons labeled with Alexa488-conjugated CTb from the PVH (PVH-CTb) were mostly distributed in middle and ventral parts of the caudal hypothalamus (Figure 3E and F) (Sawchenko and Swanson, 1983; Singru et al., 2005). Very few cells in the caudal hypothalamus were double-labeled with rMR-CTb and PVH-CTb (Figure 3C–F and Figure S4C–G).

Social defeat stress induced a remarkable expression of Fos in rMR-CTb-labeled neurons that formed a prominent cluster in the dorsal part of the DMH (dDMH), which was located in a rostral part of the DMH (Figure 3C and F_1 and Figure S4C). Quantification of Fos expression in rMR-CTb-labeled neurons in the dDMH revealed a marked activation of these neurons in stressed rats in comparison to control rats (Figure 3C and E–G and Figure S4D). Stress-induced Fos expression was also detected in some rMR-CTb-labeled neurons distributed between the mammillothalamic tract and fornix in the LH (Figure 3E and F). Among neurons labeled with PVH-CTb, prominent Fos expression following stress was found in a population clustering in the ventral part of the DMH (vDMH) (Figure 3D and F and Figure S4C). Fos expression in PVH-CTb-labeled neurons in the vDMH was markedly higher in stressed rats than in control rats (Figure 3D–G and Figure S4E). Stress-induced Fos expression was infrequent in CTb-labeled cells in the caudal sections containing the posterior hypothalamic nucleus (Figure S4F and G). These observations suggest that the DMH contains two separate groups of neurons mediating different stress responses: dDMH neurons projecting to the rMR for driving sympathetic thermogenic responses and

vDMH neurons projecting to the PVH for driving neuroendocrine responses.

Thermal Responses to Social Defeat Stress Require Activation of Neurons in the DMH

To investigate the role of the DMH in psychological stress-induced thermal responses, we examined the effect of muscimol-induced inactivation of DMH neurons on the BAT thermogenic and hyperthermic responses to social defeat stress. Bilateral nanoinjections of muscimol into the DMH (Figure 4A and B) eliminated most of the increases in T_{BAT} and T_{core} induced by social defeat stress, but did not affect basal T_{BAT} or T_{core} (Table S1). Stress following saline injections into the DMH induced increases in T_{BAT} and T_{core}, which were comparable to the responses in non-injected rats (Figures 1A and 4C–F).

Optogenetic Stimulation of DMH–rMR Projection Neurons Elicits BAT Thermogenic and Cardiovascular Responses

Our results raised the possibility that stress-activated dDMH neurons drive BAT thermogenesis through their direct projection to the rMR. To further investigate this possibility, we performed specific stimulation of DMH–rMR projection neurons using an *in vivo* optogenetic technique (Figure 5A) and examined the effects on thermogenic and cardiovascular parameters in anesthetized rats. ChIEF, an engineered channelrhodopsin variant with improved properties and kinetics, is a cationic channel that causes membrane depolarization and action potential when exposed to blue light (Lin et al., 2009). Transduction of DMH cells with ChIEF-tdTomato using adeno-associated virus (AAV) resulted in the localization of ChIEF-tdTomato in many cell bodies in the DMH as well as in their nerve endings densely distributed in the rMR

(Figure 5B and C). Repeated *in vivo* illumination of the ChIEF-tdTomato-containing nerve endings in the rMR with pulsed blue laser light consistently elicited increases in BAT sympathetic nerve activity (SNA) and T_{BAT} and also increased heart rate and arterial pressure simultaneously (Figure 5F and H and Table S2). A longer illumination of these nerve endings elicited a larger BAT thermogenesis, whose intensity was comparable to that induced by social defeat stress (Figure S5A and B). To reduce the variability in warming-induced inhibitiory effects on BAT thermogenesis (Tupone et al., 2011) among experiments, we performed photostimulation in the presence of a basal level of small ongoing BAT SNA under slightly cooled conditions. As a control, DMH cells were transduced with palGFP, a membrane-targeted form of GFP (Moriyoshi et al., 1996). As with ChIEF-tdTomato, palGFP was expressed in DMH neurons and delivered to their nerve endings in the rMR (Figure 5D and E). Pulsed laser illumination of these palGFP-containing nerve endings in the rMR did not increase BAT SNA, T_{BAT}, heart rate or arterial pressure (Figure 5G and H). Illumination of the ChIEF-tdTomato-containing nerve endings in the rMR, but not that of the palGFP-containing nerve endings, induced Fos expression in many VGLUT3-immunoreactive neurons in the rMR (Figure S5C), which are sympathetic premotor neurons controlling BAT (Nakamura et al., 2004). These results indicate that photoactivation of ChIEF in the DMH-derived nerve endings in the rMR caused activation of sympathetic premotor neurons in the rMR and elicited the thermogenic and cardiovascular responses, demonstrating that DMH–rMR direct projection neurons can drive BAT thermogenesis and cardiovascular responses that mimic the autonomic stress responses.

We have shown stress-activated, vDMH–PVH projection neurons. DMH neurons also project to the vlcPAG and this projection has been

proposed to contribute to BAT thermogenesis (Chen et al., 2002; Yoshida et al., 2005). Therefore, we examined the effects of optogenetic stimulation of DMH–PVH and DMH–vlcPAG projection neurons on the physiological parameters. Consistent with the presence of these projections, AAV transduction of DMH neurons with ChIEF-tdTomato resulted in the delivery of the proteins to many nerve endings in the PVH and vlcPAG (Figure S5D and E). However, laser illumination of these nerve endings in the PVH or vlcPAG elicited no obvious increase in BAT SNA, T_{BAT}, heart rate or arterial pressure (Figure 5H, Figure S5J and K, and Table S2).

Using this technique, we also determined whether LH–rMR projection neurons contribute to driving BAT thermogenesis and cardiovascular responses. Following AAV transduction of LH neurons including orexin neurons in the perifornical area (Figure S5F and G), ChIEF-tdTomato was detected in their nerve endings in the rMR, which were, however, fewer than those projecting from the DMH (compare Figure 5C and Figure S5H and I). Laser illumination of these LH-derived nerve endings in the rMR elicited a small increase in BAT SNA (Figure S5L and Table S2), which was significantly weaker than that elicited by photostimulation of DMH-derived nerve endings in the rMR (Figure 5H). Illumination of ChIEF-tdTomato-expressing cell bodies in the LH did not significantly increase BAT SNA (Figure S5M and Table S2). No obvious increase in T_{BAT}, heart rate or arterial pressure was evoked by photostimulation of cell bodies in the LH or their nerve endings in the rMR (Figure 5H and Figure S5L and M).

Antagonizing Glutamate Receptors in the rMR Diminishes Optogenetically Evoked BAT Thermogenic and Cardiac Responses

To determine whether the DMH–rMR projection neurons driving BAT thermogenesis and cardiovascular responses are glutamatergic, we examined the effect of antagonizing glutamate receptors in the rMR on sympathetic responses elicited by optogenetic stimulation of DMH neurons (Figure 6A). Laser illumination of ChIEF-tdTomato-expressing cell bodies in the DMH following a saline nanoinjection into the rMR (Figure 6B and C) consistently elicited increases in BAT SNA, T_{BAT}, heart rate and arterial pressure (Figure 6D and F). In contrast, following a subsequent nanoinjection of AP5/CNQX into the rMR (Figure 6B and C), neither BAT SNA nor T_{BAT} was increased by illumination of ChIEF-tdTomato-expressing DMH neurons and the increase in heart rate was significantly reduced (Figure 6E and F). Although the increase in arterial pressure by the stimulation of DMH neurons was attenuated by the AP5/CNQX injection in 4 out of 6 rats, this inhibitory effect was not statistically significant (Figure 6E and F).

Direct Glutamatergic Innervation of Sympathetic Premotor Neurons in the rMR by DMH neurons

To examine whether DMH neurons directly innervate sympathetic premotor neurons in the rMR, we performed anterograde neuronal tracing. AAV transduction of neurons in the DMH, mostly dDMH, with palGFP labeled their nerve endings in the rMR (Figure 7A–C and Figure S6). We found palGFP-labeled axon swellings in the rMR that were closely associated with VGLUT3-immunoreactive cell bodies (Figure 7B and Figure S6A). Confocal microscopy revealed that the axon swellings apposed to VGLUT3-immunoreactive cell bodies contained immunoreactivity for VGLUT2, a marker for a subset of glutamatergic neurons (Figure 7C and Figure S6B). In contrast, we detected no immunoreactivity for VGLUT1 nor vesicular GABA transporter, a

marker for GABAergic axon terminals, in palGFP-labeled axon swellings apposed to VGLUT3-immunoreactive cells in the rMR (Figure S6C and D).

DISCUSSION

This study revealed an important central neural pathway for the development of PSH, which transmits hypothalamic stress signals to the medullary sympathetic premotor neurons that drive metabolic heat production in BAT—an autonomic response driven in humans as well as in rodents under certain physiological and environmental conditions (Enerbäck, 2010). We demonstrated that the DMH and rMR mediate the psychological stress-driven sympathetic outflow to BAT for eliciting thermogenesis contributing to the development of PSH. Our functional neuroanatomy and *in vivo* optogenetic experiments showed that dDMH–rMR projection neurons are activated by stress and drive BAT thermogenic and cardiovascular responses. Based on these findings, we propose that the dDMH–rMR monosynaptic pathway transmits the psychological stress-driven hypothalamomedullary signal that drives sympathetic BAT thermogenesis for the development of PSH (Figure 7D).

The present dual thermotelemetry recordings in free-moving rats detected an immediate increase in T_{BAT} and a delayed increase in T_{core} after exposure to social defeat stress or an intracerebroventricular injection of PGE_2. This difference between the changes in T_{BAT} and T_{core}, which was also observed in our recording from anesthetized rats (Nakamura et al., 2002), clearly reflects heat production in BAT. Furthermore, a predominant part of the stress-induced increase in T_{BAT} was eliminated by propranolol, consistent with the β_3-adrenoceptor-mediated mechanism of BAT thermogenesis (Cannon and Nedergaard, 2004). These results confirm the validity of the present

thermotelemetric measurement of BAT thermogenesis as well as the major contribution of BAT thermogenesis to the development of PSH.

The BAT thermogenesis and hyperthermia induced by social defeat stress was eliminated by inactivation of neurons in the rMR. We have shown that the rMR contains sympathetic premotor neurons that control BAT thermogenesis (Nakamura et al., 2004) and are activated in response to social defeat stress (Lkhagvasuren et al., 2011). These findings strengthen the notion that psychological stress activates sympathetic premotor neurons in the rMR to drive BAT thermogenesis for the development of PSH. In addition to BAT thermogenesis, psychological stress can also induce cutaneous vasoconstriction (Ootsuka et al., 2008), an α-adrenoceptor-mediated sympathetic response, which supports the stress-induced increase in body temperature by decreasing heat dissipation from the body surface. Sympathetic premotor neurons in the rMR also multisynaptically innervate skin blood vessels as well as BAT (Nakamura et al., 2004). Therefore, some of the stress-activated sympathetic premotor neurons in the rMR likely drive cutaneous vasoconstriction, although cutaneous vasomotion was not measured in the present study. Nonetheless, the strong inhibition of PSH with a β_3-adrenoblocker (Lkhagvasuren et al., 2011) and propranolol (this study) suggests that the contribution of cutaneous vasoconstriction to social defeat stress-induced hyperthermia is minor compared to that of BAT thermogenesis.

Blockade of glutamate receptors in the rMR largely eliminated BAT thermogenesis and hyperthermia induced by social defeat stress, indicating that glutamatergic inputs to rMR neurons are important in the central sympathetic drive to elicit stress-induced BAT thermogenesis. As a candidate for the brain region that provides such glutamatergic inputs to the rMR, we focused on the caudal hypothalamus, because this

region contains the classic “defense area” (Yardley and Hilton, 1986; DiMicco et al., 2002). The DMH in the caudal hypothalamus provides numerous axonal projections to the rMR (Hosoya et al., 1987). Despite earlier efforts (Sarkar et al., 2007), the present functional neuroanatomy combining retrograde neuronal tracing with Fos immunohistochemistry is the first to map the detailed distribution of caudal hypothalamic neurons that are activated in response to psychological stress and that innervate the medullary sympathetic premotor region. This mapping revealed a cluster of stress-activated, rMR-projecting neurons in the dDMH. Our anterograde tracing allowed visualization of a close association of DMH-derived, VGLUT2-containing axon terminals with VGLUT3-expressing sympathetic premotor neurons in the rMR. Importantly, inactivation of DMH neurons eliminated stress-induced BAT thermogenesis and hyperthermia. Thus, our data demonstrate that PSH results from an activation of dDMH neurons, possibly arising from forebrain stress signals, which then provide a direct glutamatergic excitatory input to thermoregulatory sympathetic premotor neurons in the rMR to drive BAT thermogenesis (Figure 7D).

This view is further supported by several lines of anatomical and physiological evidence. Transsynaptic retrograde neuronal tracing from BAT using pseudorabies virus has shown that both rMR and DMH exhibit viral labeling and the labeling in the DMH occurs with a delay of ~12 hours from that in the rMR, which approximately corresponds to the time for the virus to migrate one synapse (Cano et al., 2003; Yoshida et al., 2003). BAT thermogenesis evoked by stimulation of DMH neurons is inhibited by blockade of glutamate receptors in the rMR, and activation of glutamate receptors in the rMR evokes BAT thermogenesis and cardiovascular responses mimicking stress responses (Cao and Morrison, 2006). However, studies with such conventional physiological and

anatomical techniques could not directly demonstrate that the DMH–rMR monosynaptic pathway drives BAT thermogenesis. Furthermore, there is a controversial view that a multisynaptic pathway from the DMH to the rMR through the vlcPAG transmits a sympathetic drive for BAT thermogenesis (Chen et al., 2002; Yoshida et al., 2005). Therefore, we used an *in vivo* optogenetic technique to perform projection site-selective stimulation of DMH-derived nerve endings. Photostimulation of DMH-derived nerve endings in the rMR elicited increases in BAT SNA and T_{BAT} accompanied with activation of sympathetic premotor neurons in the rMR. The intensity of this optogenetic activation of BAT thermogenesis was comparable to that induced by social defeat stress. Furthermore, BAT thermogenesis elicited by photostimulation of DMH cell bodies was eliminated by antagonizing glutamate receptors in the rMR. On the other hand, photostimulation of DMH-derived nerve endings in the vlcPAG showed no effect on BAT thermogenic activity. These results indicate that BAT thermogenesis can be driven by the glutamatergic monosynaptic pathway from the dDMH to the rMR, but not by the multisynaptic pathway from the DMH that involves the vlcPAG. Activation of DMH and rMR neurons is also required for sympathetic thermogenic outflows to BAT for cold defense and fever (Nakamura et al., 2002; Madden and Morrison, 2004; Nakamura et al., 2005; Nakamura and Morrison, 2007) in addition to PSH. Therefore, we propose that the dDMH–rMR direct neuronal projection constitutes the “trunk sympathetic pathway” that mediates the hypothalamomedullary BAT thermogenic drives not only for PSH, but also for basal thermoregulation and fever.

Although both DMH and rMR also play pivotal roles in cardiovascular responses to stress (Stotz-Potter et al., 1996a,b; Zaretsky et al., 2003; Pham-Le et al., 2011), the functional connection between

these sites for driving the cardiovascular stress responses has yet to be studied. Our photostimulation of DMH-derived nerve endings in the rMR elicited increases in heart rate and arterial pressure, and glutamate receptor blockade in the rMR inhibited the cardiac responses elicited by photostimulation of DMH cell bodies and by social defeat stress. Therefore, the DMH–rMR glutamatergic monosynaptic pathway likely mediates stress-driven sympathetic outflows to the heart as well as to BAT. However, the limited inhibitory effect of glutamate receptor blockade in the rMR on the pressor responses elicited by DMH photostimulation and by social defeat stress suggests that a non-glutamatergic DMH–rMR pathway may partly mediate the cardiovascular hypothalamomedullary signaling. Alternatively, in addition to the DMH–rMR projection, a projection from the DMH to the cardiovascular sympathetic premotor region, rostral ventrolateral medulla, could partly mediate the cardiovascular responses (Horiuchi et al., 2004).

Although our data demonstrate that the dDMH is the principal site in the caudal hypothalamus that mediates the stress-driven sympathetic outflow to BAT, recent studies propose that orexin neurons, which are distributed mostly in the perifornical area of the LH, are involved in BAT thermogenesis. Orexin neurons project to the rMR from the LH, but few from the DMH (Berthoud et al., 2005; Tupone et al., 2011). Orexin injection into the rMR can increase BAT thermogenesis under cooled conditions in which BAT thermogenesis is activated (Tupone et al., 2011). Genetic ablation of orexin neurons attenuates hyperthermia induced by handling stress (Zhang et al., 2010). Our CTb-Fos mapping showed that social defeat stress activates some rMR-projecting neurons in the perifornical area, which may include orexin neurons. Although these findings support the involvement of orexin neurons in the control of BAT thermogensis through their projection to the rMR, the orexin-mediated

mechanism for driving BAT thermogenesis may not be simple. Injection of a putative orexin receptor antagonist into the rMR evokes, instead of inhibiting, BAT thermogenesis (Tupone et al., 2011) and ablation of the orexin gene does not affect the PSH evoked by handling stress (Zhang et al., 2010). In the present study, optogenetic stimulation of LH neurons including orexin neurons or their nerve endings in the rMR elicited only a very limited thermogenic response in BAT even under cooled conditions with a small ongoing BAT SNA, consistent with the fewer LH-derived nerve endings in the rMR than those from the dDMH. Indeed, there is a caveat that orexin neuron-specific photostimulation might result in more intense responses. However, based on the predominance of the dDMH over the LH in stress-induced neuronal activation and in sensitivity to optogenetic stimulation, we suppose that orexin neurons play a subsidiary role in stress-induced BAT thermogenesis, for example, by modulating the DMH-derived glutamatergic input at the rMR. Orexin neurons could also contribute to the stress mechanism through their projections to diverse forebrain regions (Peyron et al., 1998).

Intriguingly, we found another set of stress-activated neurons in the vDMH, which project to the PVH, the output center for the hypothalamo-pituitary-adrenal endocrine axis. These DMH neurons were segregated from the stress-activated, rMR-projecting neurons in the dDMH. Optogenetic stimulation of DMH–PVH projection neurons did not elicit BAT thermogenesis. Inactivation of DMH neurons strongly reduces stress-induced ACTH release and Fos expression in the PVH (Stotz-Potter et al., 1996a; Morin et al., 2001), suggesting that the DMH is antecedent to the PVH in the pathway for the neuroendocrine stress response. Based on these findings, we propose that the DMH serves as a hub for the flows of central stress signals by providing the sympathetic

efferent from the dDMH to the rMR and the neuroendocrine efferent from the vDMH to the PVH (Figure 7D). Further investigation is needed to determine how these two groups of DMH neurons are activated in parallel by stress signals from antecedent neurons. PVH-projecting neurons in the vDMH are also activated by leptin (Elmquist et al., 1998), suggesting that these neurons might be responsible for neuroendocrine responses to leptin (Ahima et al., 1996) as well as to stress.

Injection of 8-OH-DPAT into the rMR inhibited stress-induced BAT thermogenesis and hyperthermia, suggesting that serotonergic inputs to the rMR or locally released serotonin can inhibit the stress responses through the inhibitory 5-HT_{1A} receptors, potentially expressed in spinally projecting sympathetic premotor neurons in the rMR (Helke et al. 1997). Hypothermia was caused by subcutaneous injection of 8-OH-DPAT, but not by injection of this drug into the rMR with the present dose. Therefore, systemically administered 5-HT_{1A} receptor agonists might cause hypothermia by acting at brain sites other than the rMR. The idea that 5-HT_{1A} receptors on different populations of neurons underlie the inhibition of PSH and the hypothermia from systemic 8-OH-DPAT is also supported by a pharmacological study using serotonin transporter knockout rats (Olivier et al., 2008).

The present study demonstrates that the dDMH–rMR monosynaptic pathway transmits a glutamatergic excitatory stress signal to drive BAT thermogenesis for the development of PSH. Considering that the mechanism of PSH may be relevant to the etiology of psychogenic fever (Oka & Oka, 2012), this pathway may also be important in the development of psychogenic fever in humans. However, the contribution of BAT thermogenesis to PSH and psychogenic fever in humans has yet to be determined. Due to the large contribution of BAT thermogenesis to whole body energy expenditure, the present finding

seems important in addressing the mental health question: how do emotional and psychological states affect metabolism? Further studies are required to reveal the central circuitries that link the forebrain stress mechanism to the autonomic and neuroendocrine systems, in which the DMH appears to play a key role. This first report of successful photostimulation of metabolic thermogenesis introduces the utility of the *in vivo* optogenetic technique for probing such central stress circuitries.

EXPERIMENTAL PROCEDURES

Animals

Wistar rats (male) and Long–Evans rats (male and female) (SLC Japan, Shizuoka, Japan) were housed with *ad libitum* access to food and water in a room air-conditioned at 24 ± 1ºC with a 12 hr light/dark cycle. All animal protocols were approved by the Animal Research Committee, Graduate School of Medicine, Kyoto University.

Social Defeat Stress and Drug Injection

Wistar rats implanted with a telemetric transmitter to measure T_{BAT} and T_{core} (Data Science International) were exposed to social defeat stress (Lkhagvasuren et al., 2011; see Supplemental Experimental Procedures). After 60 min of the stress exposure, the rats were returned to their home cage. In experiments to examine the effects of drugs on stress responses, the rats received an intravenous, subcutaneous or intracranial injection of saline or drugs 5 min before the stress exposure. Propranolol (5 mg/kg, 300 µl) was injected into the jugular vein. 8-OH-DPAT (0.5 mg/kg, 300 µl) was injected subcutaneously in the lower back. Muscimol (1 mM), 8-OH-DPAT (10 mM) and AP5/CNQX (10 mM each) were nanoinjected (100 nl) into the rMR and muscimol was bilaterally nanoinjected (100 nl per side) into the DMH. The doses for the intracranial injections are in

the ranges used in anesthetized rats (Nakamura and Morrison, 2007). The intravenous and intracranial injections were made through preimplanted cannulae. To reduce the number of animals used, some rats were exposed to stress twice at an interval of > 1 week. Our preliminary experiments showed that thermal responses induced by stress exposures repeated at this interval were comparable. The first stress exposure was always for testing saline and the second one was for testing one of the drugs, which was given at the same site through the same administration route as the saline injection. At the end of the experiment, the rats that received brain injections received another injection at the same site with 50 nl of fluorescent microspheres (Invitrogen) to label the injection sites. The rats were anesthetized and transcardially perfused with 4% formaldehyde in 0.1 M phosphate buffer (pH 7.4). The injection sites were identified in the brain sections.

Retrograde Neuronal Tracing

Retrograde neuronal tracing combined with Fos immunohistochemistry followed our method (Nakamura and Morrison, 2008). Anesthetized Wistar rats received injections of Alexa488- and Alexa594-conjugated CTb (Invitrogen) into the right PVH and the rMR, respectively. One week later, the rats were exposed to social defeat stress for 60 min or received a control handling, which allowed them to be in their home cages for 60 min, but were provided with a gentle lift of the tail at the beginning and end of the period (Lkhagvasuren et al., 2011). Fifteen minutes after the end of the stress or control period, they were anesthetized and perfused with 4% formaldehyde. The brains were cut into 30-µm-thick frontal sections and subjected to immunohistochemistry.

***In Vivo* Optogenetic Stimulation**

Anesthetized Wistar rats received a unilateral injection into the DMH or LH with AAV-CMV-ChIEF-tdTomato or AAV-CMV-palGFP. One week later, they were subjected to *in vivo* physiological recordings under urethane and α-chloralose anesthesia as described (Nakamura and Morrison, 2007). To illuminate cell bodies or nerve endings, an optical fiber (diameter, 200 μm; Thorlabs) was perpendicularly inserted into the brain so that the fiber tip was positioned at 0.5–1.0 mm dorsal to the target site. The light source was a diode-pumped 445 nm blue laser (Power technology) controlled by an electrical stimulator that generated pulse signals. The power output was measured at the fiber tip with a light meter beforehand and preset at 8 mW (when the laser was activated in a continuous mode). The target sites were illuminated with 50-ms light pulses at 10 Hz. Each train of the light pulses was given for 30 sec or 180 sec. In some experiments, AP5/CNQX (5 mM each, 60 nl) or saline was injected into the rMR.

Immunohistochemistry

Immunohistochemistry followed our methods (Nakamura et al., 2004, 2005). The primary antibodies used are anti-c-Fos rabbit serum (Ab-5; Calbiochem), anti-mRFP rabbit antibody (Hioki et al., 2010), anti-GFP rabbit antibody (Tamamaki et al., 2000), anti-GFP mouse antibody (Invitrogen), anti-VGLUT1 rabbit antibody (Hioki et al., 2003), anti-VGLUT2 rabbit antibody (Hioki et al., 2003), anti-VGLUT3 guinea pig antibody (Hioki et al., 2004), anti-vesicular GABA transporter rabbit antibody (Chemicon) and anti-orexin-A goat antibody (Santa Cruz). The anti-mRFP antibody shows reactivity to tdTomato.

Anatomy and Statistical Analysis

The anatomical nomenclature followed Paxinos and Watson's stereotaxic rat brain atlas (Paxinos and Watson, 2007), except that for nomenclature purposes, the raphe pallidus nucleus was divided into two parts: rostral and caudal to the rostral end of the inferior olivary complex (Nakamura et al., 2002).

Data are shown as the means ± SEM. Differences between groups were examined by a two-tailed paired or unpaired *t*-test or by a one-way or two-way ANOVA followed by Bonferroni's *post-hoc* test as appropriate. $P < 0.05$ was considered statistically significant.

SUPPLEMENTAL INFORMATION

Supplemental Information includes 6 figures, 2 tables and Supplemental Experimental Procedures and can be found with this article online at http:// dx.doi.org/10.1016/j.cmet.2014.05.018.

ACKNOWLEDGMENTS

We thank Chika Tanizawa for anatomical assistance, Shaun F. Morrison for critical reading of the manuscript, and Yoshie Nakagawa for assistance with manuscript preparation. This study was supported by the Funding Program for Next Generation World-Leading Researchers from the Japan Society for the Promotion of Science (LS070 to K.N.), by Grants-in-Aid for Scientific Research (21890114, 22689007, 26118508 and 26713009 to K.N., 23115101 and 25250006 to T.K., 24500408 and 25123709 to H.H., and 24790233 to N.K.) and a Special Coordination Fund for Promoting Science and Technology (to K.N.) from the MEXT of Japan, and by grants from the Nakajima Foundation, Takeda Science Foundation and Kowa Life Science Foundation (to K.N.).

REFERENCES

Ahima, R.S., Prabakaran, D., Mantzoros, C., Qu, D., Lowell, B., Maratos-Flier, E., and Flier, J.S. (1996). Role of leptin in the neuroendocrine response to fasting. Nature *382*, 250–252.

Berthoud, H.R., Patterson, L.M., Sutton, G.M., Morrison, C., and Zheng, H. (2005). Orexin inputs to caudal raphé neurons involved in thermal, cardiovascular, and gastrointestinal regulation. Histochem. Cell Biol. *123*, 147–156.

Bishop, D. (2003). Warm up I: potential mechanisms and the effects of passive warm up on exercise performance. Sports Med. *33*, 439–454.

Björkqvist, K. (2001). Social defeat as a stressor in humans. Physiol. Behav. *73*, 435–442.

Cannon, B., and Nedergaard, J. (2004). Brown adipose tissue: function and physiological significance. Physiol. Rev. *84*, 277–359.

Cano, G., Passerin, A.M., Schiltz, J.C., Card, J.P., Morrison, S.F., and Sved, A.F. (2003). Anatomical substrates for the central control of sympathetic outflow to interscapular adipose tissue during cold exposure. J. Comp. Neurol. *460*, 303–326.

Cao, W.H., and Morrison, S.F. (2006). Glutamate receptors in the raphe pallidus mediate brown adipose tissue thermogenesis evoked by activation of dorsomedial hypothalamic neurons. Neuropharmacology *51*, 426–437.

Chen, X.M., Nishi, M., Taniguchi, A., Nagashima, K., Shibata, M., and Kanosue, K. (2002). The caudal periaqueductal gray participates in the activation of brown adipose tissue in rats. Neurosci. Lett. *331*, 17–20.

DiMicco, J.A., Samuels, B.C., Zaretskaia, M.V., and Zaretsky, D.V. (2002). The dorsomedial hypothalamus and the response to stress: part renaissance, part revolution. Pharmacol. Biochem. Behav. *71*, 469–480.

Elmquist, J.K., Ahima, R.S., Elias, C.F., Flier, J.S., and Saper, C.B. (1998). Leptin activates distinct projections from the dorsomedial and ventromedial hypothalamic nuclei. Proc. Natl. Acad. Sci. U. S. A. *95*, 741–746.

Enerbäck, S. (2010). Human brown adipose tissue. Cell Metab. *11*, 248–252.

Helke, C.J., Capuano, S., Tran, N., and Zhuo, H. (1997). Immunocytochemical studies of the 5-HT_{1A} receptor in ventral medullary neurons that project to the intermediolateral cell column and contain serotonin or tyrosine hydroxylase immunoreactivity. J. Comp. Neurol. *379*, 261–270.

Hermann, D.M., Luppi, P.H., Peyron, C., Hinckel, P., and Jouvet, M. (1997). Afferent projections to the rat nuclei raphe magnus, raphe pallidus and reticularis gigantocellularis pars α demonstrated by iontophoretic application of choleratoxin (subunit b). J. Chem. Neuroanat. *13*, 1–21.

Hioki, H., Fujiyama, F., Nakamura, K., Wu, S.X., Matsuda, W., and Kaneko, T. (2004). Chemically specific circuit composed of vesicular glutamate transporter 3- and preprotachykinin B-producing interneurons in the rat neocortex. Cereb. Cortex *14*, 1266–1275.

Hioki, H., Fujiyama, F., Taki, K., Tomioka, R., Furuta, T., Tamamaki, N., and Kaneko, T. (2003). Differential distribution of vesicular glutamate transporters in the rat cerebellar cortex. Neuroscience *117*, 1–6.

Hioki, H., Nakamura, H., Ma, Y.F., Konno, M., Hayakawa, T., Nakamura, K.C., Fujiyama, F., and Kaneko, T. (2010). Vesicular glutamate transporter 3-expressing nonserotonergic projection neurons constitute a subregion in the rat midbrain raphe nuclei. J. Comp. Neurol. *518*, 668–686.

Hjorth, S. (1985). Hypothermia in the rat induced by the potent serotoninergic agent 8-OH-DPAT. J. Neural. Transm. *61*, 131–135.

Horiuchi, J., McAllen, R.M., Allen, A.M., Killinger, S., Fontes, M.A.P., and Dampney, R.A.L. (2004). Descending vasomotor pathways from the dorsomedial hypothalamic nucleus: role of medullary raphe and RVLM. Am. J. Physiol. Regul. Integr. Comp. Physiol. *287*, R824–R832.

Hosoya, Y., Ito, R., and Kohno, K. (1987). The topographical organization of neurons in the dorsal hypothalamic area that project to the spinal cord or to the nucleus raphé pallidus in the rat. Exp. Brain Res. *66*, 500–506.

Lin, J.Y., Lin, M.Z., Steinbach, P., and Tsien, R.Y. (2009). Characterization of engineered channelrhodopsin variants with improved propertiesand kinetics. Biophys. J. *96*, 1803–1814.

Lkhagvasuren, B., Nakamura, Y., Oka, T., Sudo, N., and Nakamura, K. (2011). Social defeat stress induces hyperthermia through activation of thermoregulatory sympathetic premotor neurons in the medullary raphe region. Eur. J. Neurosci. *34*, 1442–1452.

Madden, C.J., and Morrison, S.F. (2004). Excitatory amino acid receptors in the dorsomedial hypothalamus mediate prostaglandin-evoked thermogenesis in brown adipose tissue. Am. J. Physiol. Regul. Integr. Comp. Physiol. *286*, R320–R325.

Morin, S.M., Stotz-Potter, E.H., and DiMicco, J.A. (2001). Injection of muscimol in dorsomedial hypothalamus and stress-induced Fos expression in paraventricular nucleus. Am. J. Physiol. Regul. Integr. Comp. Physiol. *280*, R1276–R1284.

Moriyoshi, K., Richards, L.J., Akazawa, C., O'Leary, D.D.M., and Nakanishi, S. (1996). Labeling neural cells using adenoviral gene transfer of membrane-targeted GFP. Neuron *16*, 255–260.

Morrison, S.F. (2004). Activation of 5-HT_{1A} receptors in raphe pallidus inhibits leptin-evoked increases in brown adipose tissue thermogenesis. Am. J. Physiol. Regul. Integr. Comp. Physiol. *286*, R832–R837.

Nakamura, K. (2011). Central circuitries for body temperature regulation and fever. Am. J. Physiol. Regul. Integr. Comp. Physiol. *301*, R1207–R1228.

Nakamura, K., Matsumura, K., Hübschle, T., Nakamura, Y., Hioki, H., Fujiyama, F., Boldogköi, Z., König, M., Thiel, H.J., Gerstberger, R., et al. (2004). Identification of sympathetic premotor neurons in medullary raphe regions mediating fever and other thermoregulatory functions. J. Neurosci. *24*, 5370–5380.

Nakamura, K., Matsumura, K., Kaneko, T., Kobayashi, S., Katoh, H., and Negishi, M. (2002). The rostral raphe pallidus nucleus mediates pyrogenic transmission from the preoptic area. J. Neurosci. *22*, 4600–4610.

Nakamura, K., and Morrison, S.F. (2007). Central efferent pathways mediating skin cooling-evoked sympathetic thermogenesis in brown adipose tissue. Am. J. Physiol. Regul. Integr. Comp. Physiol. *292*, R127–R136.

Nakamura, K., and Morrison, S.F. (2008) A thermosensory pathway that controls body temperature. Nat. Neurosci. *11*, 62–71.

Nakamura, Y., Nakamura, K., Matsumura, K., Kobayashi, S., Kaneko, T., and Morrison, S.F. (2005). Direct pyrogenic input from prostaglandin EP3 receptor-expressing preoptic neurons to the dorsomedial hypothalamus. Eur. J. Neurosci. *22*, 3137–3146.

Nozu, T., and Uehara, A. (2005). The diagnoses and outcomes of patients complaining of fever without any abnormal findings on diagnostic tests. Intern. Med. *44*, 901–902.

Oka, T., and Oka, K. (2012). Mechanisms of psychogenic fever. Adv. Neuroimmune Biol. *3*, 3–17.

Olivier, J.D.A., Cools, A.R., Olivier, B., Homberg, J.R., Cuppen, E., and Ellenbroek, B.A. (2008). Stress-induced hyperthermia and basal body temperature are mediated by different 5-HT_{1A} receptor populations: a study in SERT knockout rats. Eur. J. Pharmacol. *590*, 190–197.

Ootsuka, Y., Blessing, W.W., and Nalivaiko, E. (2008). Selective blockade of 5-HT2A receptors attenuates the increased temperature response in brown adipose tissue to restraint stress in rats. Stress *11*, 125–133.

Paxinos, G., and Watson, C. (2007). The Rat Brain in Stereotaxic Coordinates, 6th edn. (San Diego: Academic Press).

Peyron, C., Tighe, D.K., van den Pol, A.N., de Lecea, L., Heller, H.C., Sutcliffe, J.G., and Kilduff, T.S. (1998). Neurons containing hypocretin (orexin) project to multiple neuronal systems. J. Neurosci. *18*, 9996–10015.

Pham-Le, N.M., Cockburn, C., Nowell, K., and Brown, J. (2011). Activation of $GABA_A$ or $5HT_{1A}$ receptors in the raphé pallidus abolish the cardiovascular responses to exogenous stress in conscious rats. Brain Res. Bull. *86*, 360–366.

Sagar, S.M., Sharp, F.R., and Curran, T. (1988). Expression of *c-fos* protein in brain: metabolic mapping at the cellular level. Science *240*, 1328–1331.

Saper, C.B., Romanovsky, A.A., and Scammell, T.E. (2012). Neural circuitry engaged by prostaglandins during the sickness syndrome. Nat. Neurosci. *15*, 1088–1095.

Sarkar, S., Zaretskaia, M.V., Zaretsky, D.V., Moreno, M., and DiMicco, J.A. (2007). Stress- and lipopolysaccharide-induced c-fos expression and nNOS in hypothalamic neurons projecting to medullary raphe in

rats: a triple immunofluorescent labeling study. Eur. J. Neurosci. *26*, 2228–2238.

Sawchenko, P.E., and Swanson, L.W. (1983). The organization of forebrain afferents to the paraventricular and supraoptic nuclei of the rat. J. Comp. Neurol. *218*, 121–144.

Singru, P.S., Fekete, C., and Lechan, R.M. (2005). Neuroanatomical evidence for participation of the hypothalamic dorsomedial nucleus (DMN) in regulation of the hypothalamic paraventricular nucleus (PVN) by α-melanocyte stimulating hormone. Brain Res. *1064*, 42–51.

Stotz-Potter, E.H., Morin, S.M., and DiMicco, J.A. (1996a). Effect of microinjection of muscimol into the dorsomedial or paraventricular hypothalamic nucleus on air stress-induced neuroendocrine and cardiovascular changes in rats. Brain Res. *742*, 219–224.

Stotz-Potter, E.H., Willis, L.R., and DiMicco, J.A. (1996b). Muscimol acts in dorsomedial but not paraventricular hypothalamic nucleus to suppress cardiovascular effects of stress. J. Neurosci. *16*, 1173–1179.

Tamamaki, N., Nakamura, K., Furuta, T., Asamoto, K., and Kaneko, T. (2000). Neurons in Golgi-stain-like images revealed by GFP-adenovirus infection in vivo. Neurosci. Res. *38*, 231–236.

Timmerman, R.J., Thompson, J., Noordzij, H.M., and van der Meer, J.W. (1992). Psychogenic periodic fever. Neth. J. Med. *41*, 158–160.

Tupone, D., Madden, C.J., Cano, G., and Morrison, S.F. (2011). An orexinergic projection from perifornical hypothalamus to raphe pallidus increases rat brown adipose tissue thermogenesis. J. Neurosci. *31*, 15944–15955.

Vinkers, C.H., Groenink, L., van Bogaert, M.J.V., Westphal, K.G.C., Kalkman, C.J., van Oorschot, R., Oosting, R.S., Olivier, B., and Korte, S.M. (2009). Stress-induced hyperthermia and infection-induced fever: two of a kind? Physiol. Behav. *98*, 37–43.

Yardley, C.P., and Hilton, S.M. (1986). The hypothalamic and brainstem areas from which the cardiovascular and behavioural components of the defence reaction are elicited in the rat. J. Auton. Nerv. Syst. *15*, 227–244.

Yoshida, K., Konishi, M., Nagashima, K., Saper, C.B., and Kanosue, K. (2005). Fos activation in hypothalamic neurons during cold or warm exposure: projections to periaqueductal gray matter. Neuroscience 133, 1039–1046.

Yoshida, K., Nakamura, K., Matsumura, K., Kanosue, K., König, M., Thiel, H.J., Boldogköi, Z., Toth, I., Roth, J., Gerstberger, R., et al. (2003). Neurons of the rat preoptic area and the raphe pallidus nucleus innervating the brown adipose tissue express the prostaglandin E receptor subtype EP3. Eur. J. Neurosci. *18*, 1848–1860.

Zaretsky, D.V., Zaretskaia, M.V., Samuels, B.C., Cluxton, L.K., and DiMicco, J.A. (2003). Microinjection of muscimol into raphe pallidus suppresses tachycardia associated with air stress in conscious rats. J. Physiol. *546*, 243–250.

Zhang, W., Sunanaga, J., Takahashi, Y., Mori, T., Sakurai, T., Kanmura, Y., and Kuwaki, T. (2010). Orexin neurons are indispensable for stress-induced thermogenesis in mice. J. Physiol. *588*, 4117–4129.

FIGURE LEGENDS

Figure 1. Social Defeat Stress Induces β-Adrenoceptor-Dependent BAT Thermogenesis and Hyperthermia

(A and B) Changes in T_{BAT} and T_{core} induced by social defeat stress (indicated by horizontal bars). Changes from the temperature at time 0 are shown (n = 6). Temperature changes for 5 min after the beginning of the stress exposure are expanded in (B).

(C–F) Effect of propranolol on social defeat stress-induced changes in T_{BAT} (C and D) and T_{core} (E and F) (n = 5). Temperature changes from the baseline, which is the average during 30 min before stress exposure, are shown in (C) and (E) (analyzed by two-way ANOVA followed by Bonferroni's *post-hoc* test). Area under the curve (AUC) during the stress period is shown in (D) and (F) (analyzed by unpaired *t*-test). $^{**}P < 0.01$, $^{***}P < 0.001$. All values are means ± SEM.

Figure 2. Inactivation of Neurons or Blockade of Glutamate Receptors in the rMR Suppresses Social Defeat Stress-Induced BAT Thermogenesis and Hyperthermia

(A–C) Nanoinjection sites in the rMR are mapped in (A) and (B). Each injection site was labeled with fluorescent microspheres (arrow in (C)). py, pyramidal tract; RMg, raphe magnus nucleus; rRPa, rostral raphe pallidus nucleus. Scale bar, 500 μm.

(D–K) Effect of muscimol (D–G) or AP5/CNQX (H–K) nanoinjection into the rMR on social defeat stress-induced changes in T_{BAT} (D, E, H and I) and T_{core} (F, G, J and K) (n = 5). Temperature changes from the baseline are shown in (D), (F), (H) and (J) (analyzed by two-way ANOVA followed by Bonferroni's *post-hoc* test). AUC during the stress period is shown in (E), (G), (I) and (K) (analyzed by unpaired *t*-

test). *P < 0.05, **P < 0.01, ***P < 0.001. All values are means ± SEM.

Figure 3. Social Defeat Stress Activates rMR-Projecting Neurons and PVH-Projecting Neurons in the DMH

(A and B) Sites of injections of Alexa594-conjugated CTb (red) into the rMR (A) and Alexa488-conjugated CTb (green) into the PVH (B). Scale bars, 300 μm. See also Figure S4A and B.

(C and D) Fos immunoreactivity in CTb-labeled cells (arrows) in the dDMH (C) and vDMH (D) following social defeat stress. Scale bars, 30 μm. See also Figure S4C–E.

(E and F) Distribution of rMR-CTb-labeled cells (red) and PVH-CTb-labeled cells (green) with or without Fos immunoreactivity in the caudal hypothalamus of control (E) and stressed rats (F). Open and filled circles indicate cells negative and positive for Fos immunoreactivity, respectively. Very few cells were double-labeled with rMR-CTb and PVH-CTb (indicated by black circles). 3V, third ventricle; Arc, arcuate nucleus; cDMH, compact part of the DMH; f, fornix; ic, internal capsule; mt, mammillothalamic tract; ot, optic tract; VMH, ventromedial hypothalamic nucleus. Scale bar, 500 μm. See also Figure S4F and G.

(G) Percentage of Fos-immunoreactive cells in CTb-labeled populations in the dDMH and vDMH (analyzed by unpaired *t*-test). **P < 0.01, ***P < 0.001. All values are means ± SEM.

Figure 4. Inactivation of DMH Neurons Eliminates Social Defeat Stress-Induced BAT Thermogenesis and Hyperthermia

(A and B) Nanoinjection sites in the DMH are mapped in (A). All rats were exposed to two stress trials at an interval of > 1 week: in the first, saline was injected bilaterally in the DMH and in the second, muscimol

was injected bilaterally (see Experimental Procedures). The positions of the injection cannulae were the same in both trials. The right side of the symmetric bilateral injection sites is shown. Each injection site was labeled with fluorescent microspheres (arrow in (B)). Scale bar, 500 μm.
(C–F) Effect of muscimol nanoinjection into the DMH on social defeat stress-induced changes in T_{BAT} (C and D) and T_{core} (E and F) (n = 5). Temperature changes from the baseline are shown in (C) and (E) (analyzed by two-way ANOVA followed by Bonferroni's *post-hoc* test). AUC during the stress period is shown in (D) and (F) (analyzed by paired *t*-test). $^{*}P < 0.05$, $^{**}P < 0.01$. All values are means ± SEM.

Figure 5. Optogenetic Stimulation of DMH–rMR Projection Neurons Elicits BAT Thermogenesis and Cardiovascular Responses

(A) *In vivo* optogenetic experiment to selectively stimulate DMH-derived nerve endings in the rMR (DMH –> rMR*; asterisk indicating the place of illumination).

(B–E) Cell bodies transduced with ChIEF-tdTomato (B, inset) and palGFP (D, inset) in the DMH (mapped with circles) and their nerve endings containing ChIEF-tdTomato (C) and palGFP (E) in the rMR. Dotted lines in (C) and (E) indicate the location of fiber optic insertion. Scale bars, 500 μm (B and D); 30 μm (insets); 100 μm (C and E).

(F and G) Effect of laser illumination of DMH-derived, ChIEF-tdTomato- (F) or palGFP-containing (G) nerve endings in the rMR on BAT thermogenic and cardiovascular activities. Horizontal bars, 30 sec. AP, arterial pressure; HR, heart rate.

(H) Changes in physiological parameters induced by illumination of DMH-derived (DMH –>) or LH-derived (LH –>) nerve endings in the rMR (rMR*), PVH (PVH*) or vlcPAG (vlcPAG*) or by illumination of cell bodies in the LH (LH cell body*) (n = 5 except DMH –> PVH* (n =

4)). Data were analyzed by one-way ANOVA followed by Bonferroni's *post-hoc* test. $*P < 0.05$, $**P < 0.01$, $***P < 0.001$. All values are means ± SEM. See also Figures S5.

Figure 6. BAT Thermogenic and Cardiac Responses to Optogenetic Stimulation of DMH Neurons Are Dependent on Glutamate Receptors in the rMR

(A) *In vivo* experiment to examine the effect of antagonizing glutamate receptors in the rMR on physiological responses to photostimulation of DMH neurons (DMH cell body*).

(B and C) Nanoinjection sites in the rMR are mapped in (B). Each circle indicates a site of saline and AP5/CNQX injections made at the same location in each rat. The effect of saline was always tested first. Each injection site was labeled with fluorescent microspheres (arrow in (C)). Scale bar, 500 μm.

(D and E) Effect of illumination of ChIEF-tdTomato-expressing cells in the DMH on BAT thermogenic and cardiovascular activities following saline (D) or AP5/CNQX injection (E) into the rMR. Results from the same rat are shown. Horizontal bars, 30 sec.

(F) Changes in physiological parameters induced by photostimulation of DMH cell bodies following saline or AP5/CNQX injection into the rMR ($n = 6$). Data were analyzed by paired *t*-test. $*P < 0.05$, $**P < 0.01$, $***P < 0.001$. All values are means ± SEM.

Figure 7. DMH-Derived, VGLUT2-Containing Nerve Endings Are Closely Associated with Sympathetic Premotor Neurons in the rMR

(A) AAV transduction of DMH neurons with palGFP. Scale bar, 500 μm.

(B) A bright field image of palGFP-labeled axon swellings (arrowheads) apposed to a VGLUT3-immunoreactive cell body in the rMR. Scale bar, 10 μm.

(C) A pseudocolored confocal image of VGLUT2-immunoreactive, palGFP-labeled axon swellings (arrowheads) apposed to a VGLUT3-immunoreactive cell body (asterisk) in the rMR. Scale bar, 10 μm. See also Figure S6.

(D) Schematic central circuits for sympathetic and neuroendocrine stress responses. Forebrain stress signals activate two groups of DMH neurons: dDMH neurons provide a direct glutamatergic input to sympathetic premotor neurons in the rMR to drive BAT thermogenesis contributing to PSH, and vDMH neurons provide a direct input to the PVH to drive a neuroendocrine outflow to release stress hormones. Plus signs indicate excitatory neurotransmission. IML, intermediolateral nucleus.

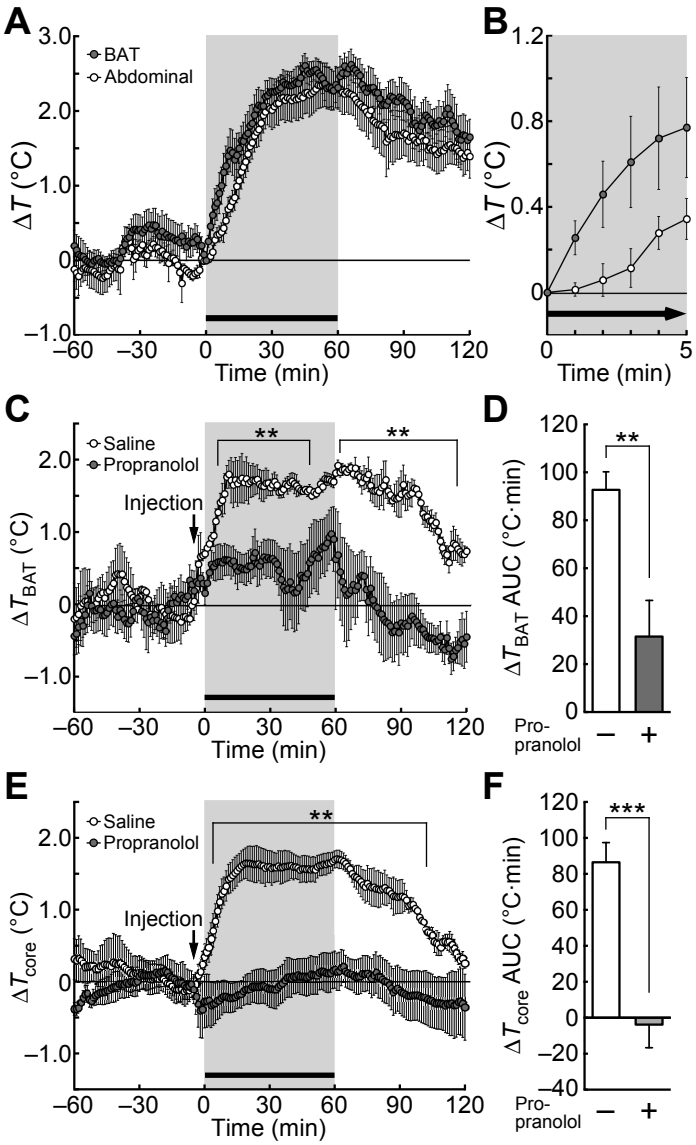

Figure 1. Kataoka *et al.*
Cell Metabolism

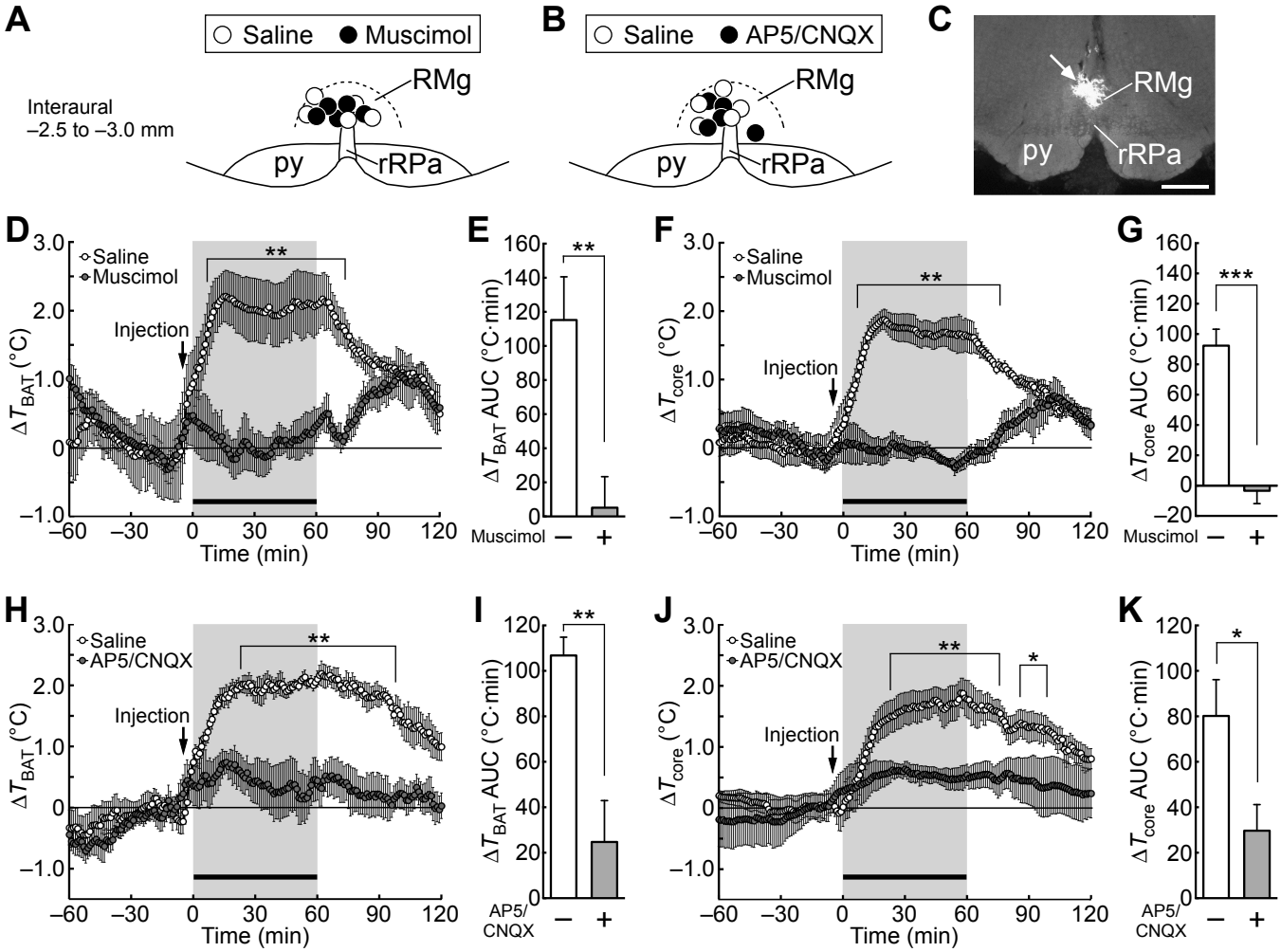

Figure 2. Kataoka *et al.*
Cell Metabolism

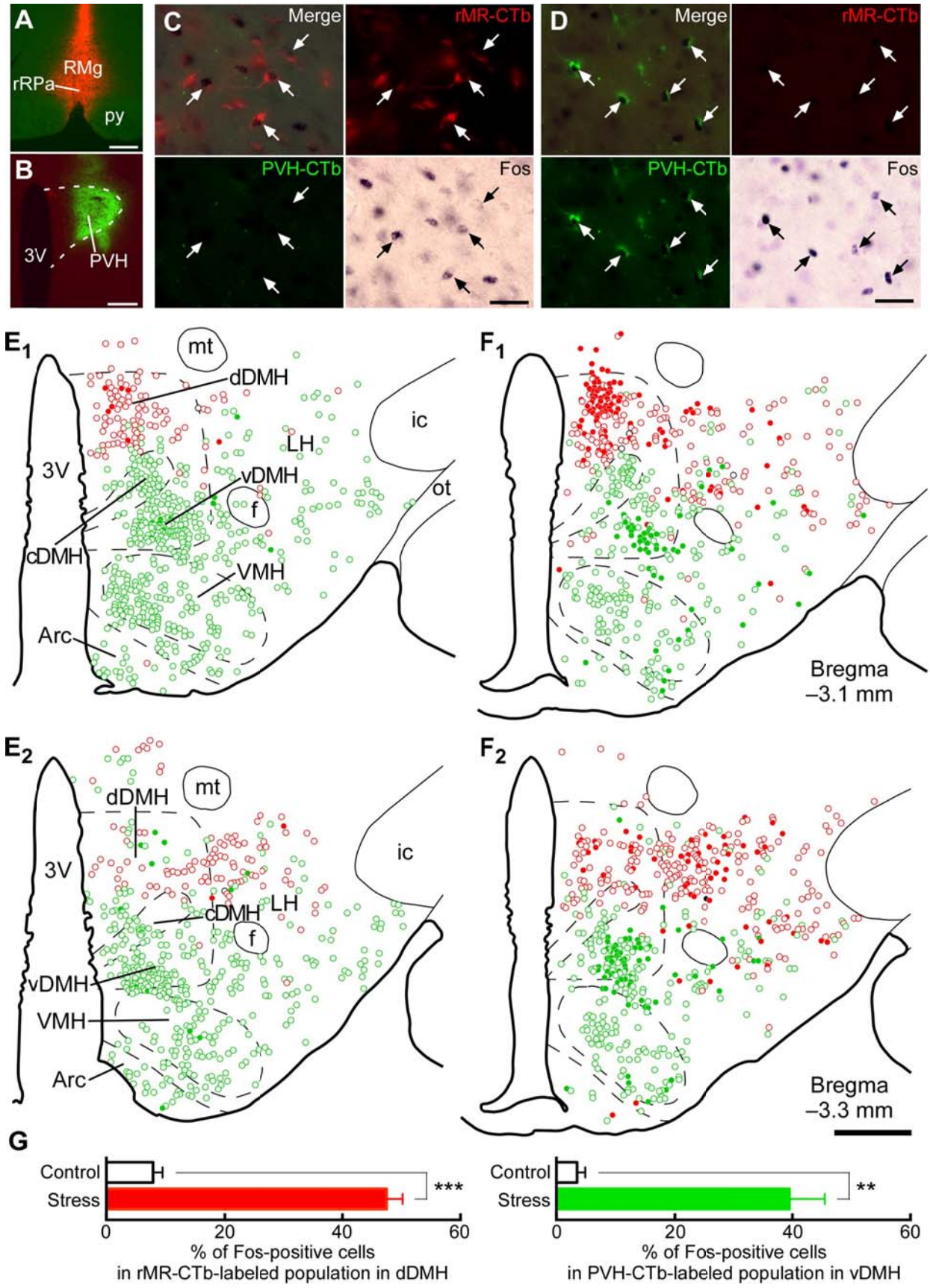

Figure 3. Kataoka *et al.*
Cell Metabolism

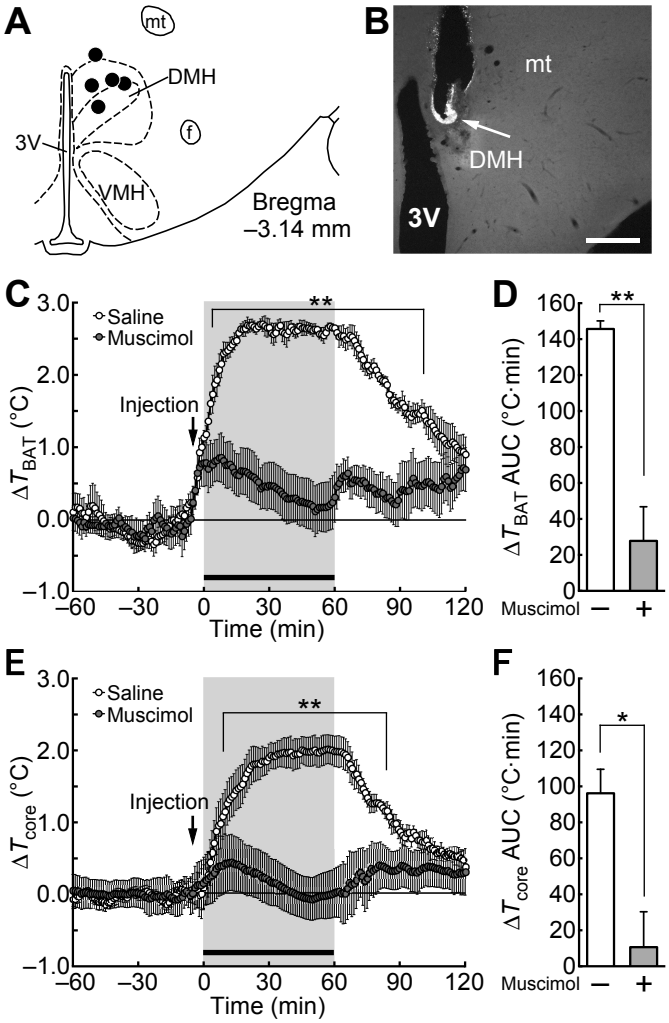

Figure 4. Kataoka *et al.*
Cell Metabolism

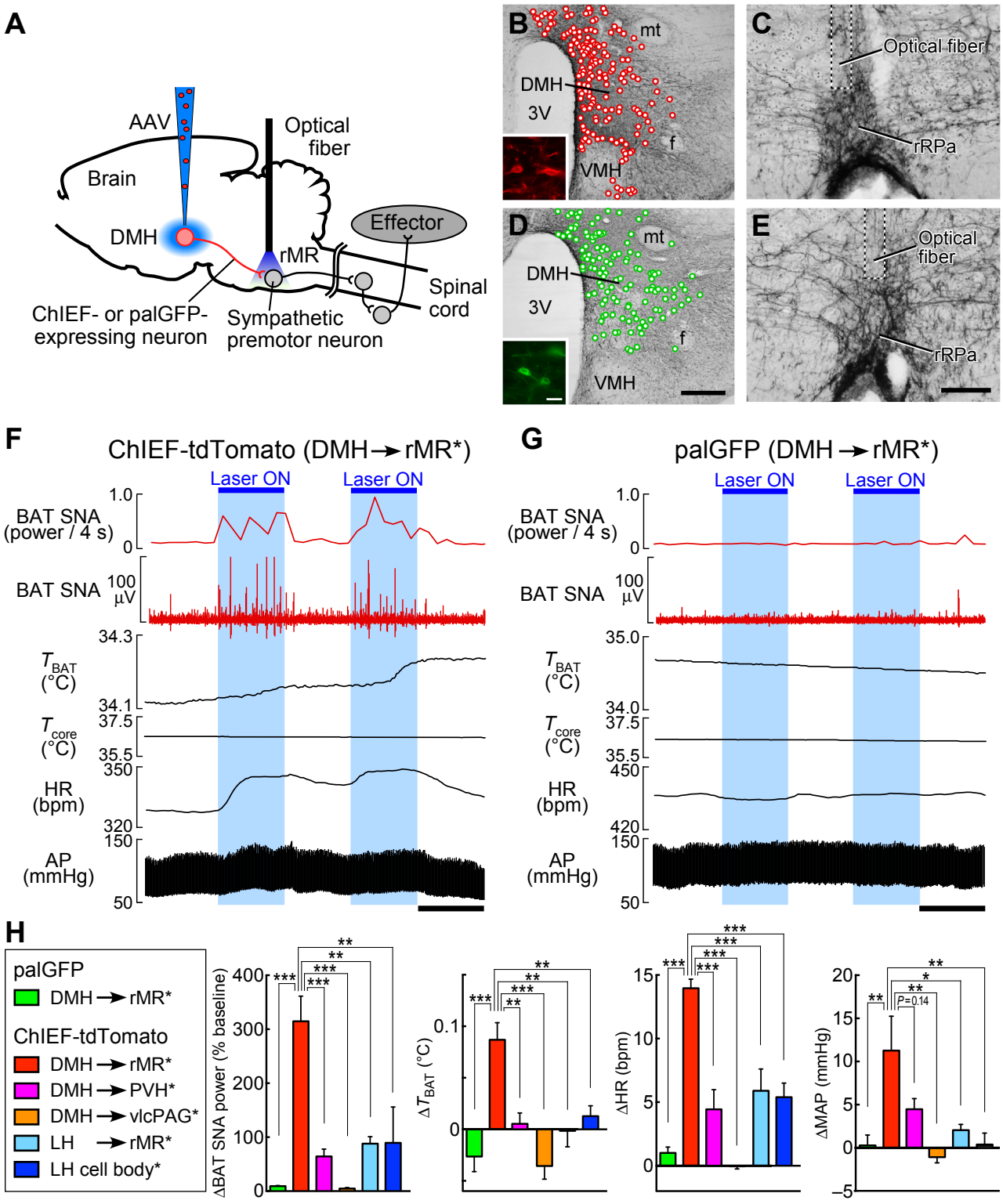

Figure 5. Kataoka *et al.*
Cell Metabolism

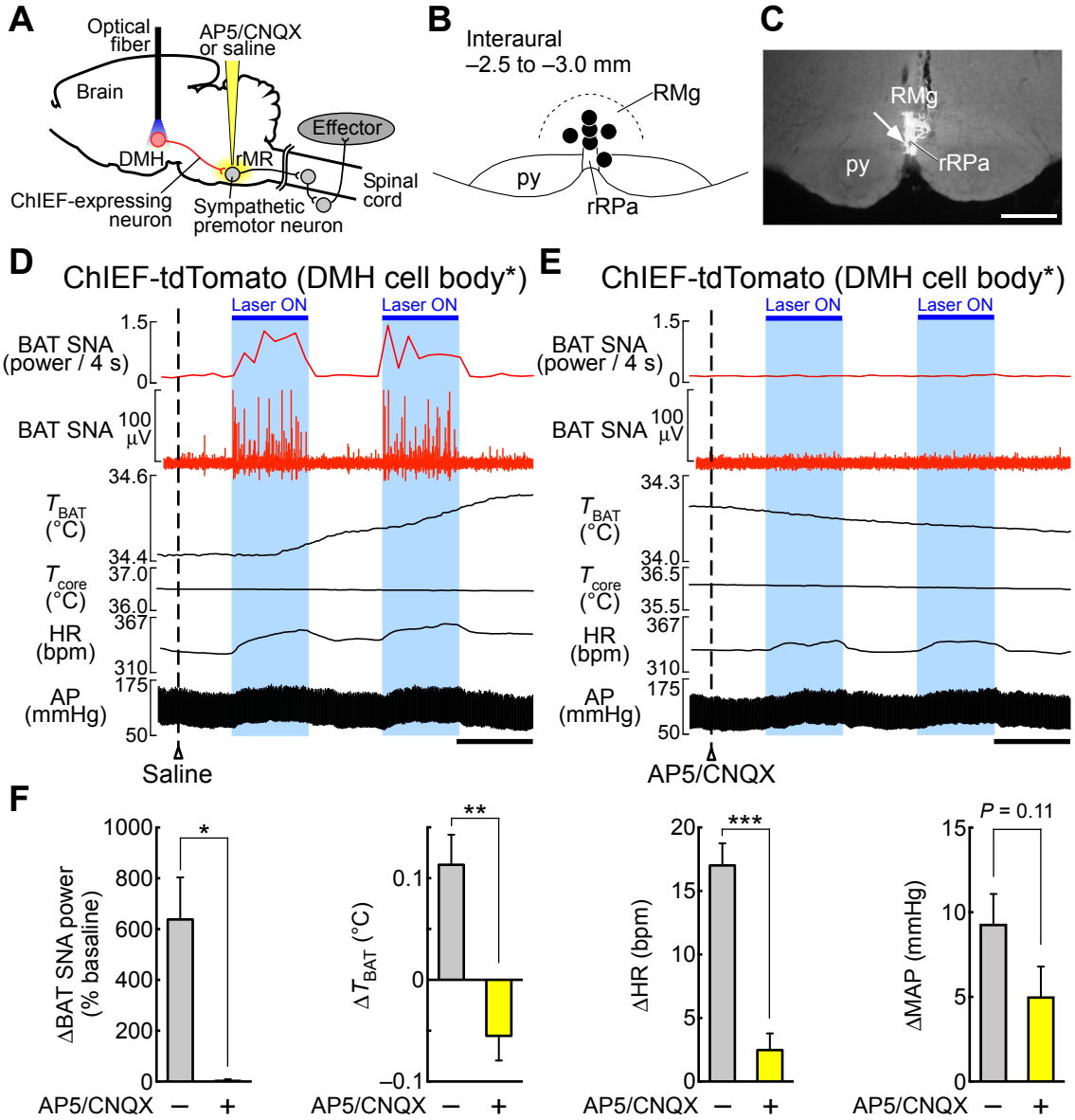

Figure 6. Kataoka *et al.*
Cell Metabolism

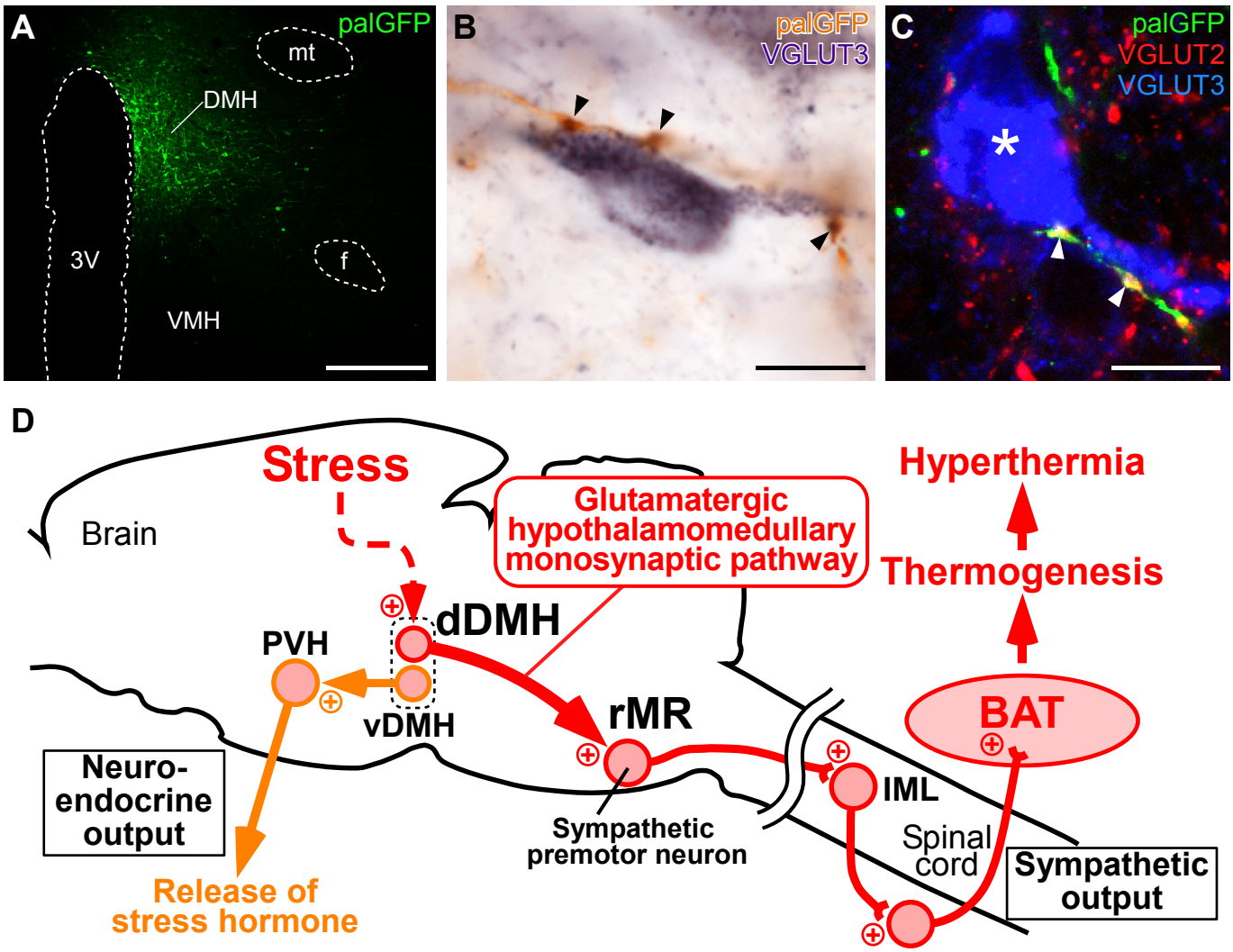

Figure 7. Kataoka *et al.*
Cell Metabolism